HHS Public Access

Author manuscript

Neurobiol Dis. Author manuscript; available in PMC 2020 May 08.

Published in final edited form as:

Neurobiol Dis. 2020 February ; 134: 104708. doi:10.1016/j.nbd.2019.104708.

Behavioral defects associated with amygdala and cortical dysfunction in mice with seeded α-synuclein inclusions

Lindsay E. Stoyka, **Andrew E. Arrant**, **Drake R. Thrasher**, **Dreson L. Russell**, **Jennifer Freire**, **Casey L. Mahoney**, **Ashwin Narayanan**, **Aseel G. Dib**, **David G. Standaert**, **Laura A. Volpicelli-Daley***

Center for Neurodegeneration and Experimental Therapeutics, University of Alabama at Birmingham, Birmingham, AL, USA

Abstract

Parkinson's disease (PD) is defined by motor symptoms such as tremor at rest, bradykinesia, postural instability, and stiffness. In addition to the classical motor defects that define PD, up to 80% of patients experience cognitive changes and psychiatric disturbances, referred to as PD dementia (PDD). Pathologically, PD is characterized by loss of dopaminergic neurons in the substantia nigra pars compacta (SNpc) and intracellular inclusions, called Lewy bodies and Lewy neurites, composed mostly of α-synuclein. Much of PD research has focused on the role of α-synuclein aggregates in degeneration of SNpc dopamine neurons because of the impact of loss of striatal dopamine on the classical motor phenotypes. However, abundant Lewy pathology is also found in other brain regions including the cortex and limbic brain regions such as the amygdala, which may contribute to non-motor phenotypes. Little is known about the consequences of α-synuclein inclusions in these brain regions, or in neuronal subtypes other than dopamine neurons. This project expands knowledge on how α-synuclein inclusions disrupt behavior, specifically non-motor symptoms of synucleinopathies. We show that bilateral injections of fibrils into the striatum results in robust bilateral α-synuclein inclusion formation in the cortex and amygdala. Inclusions in the amygdala and prefrontal cortex primarily localize to excitatory neurons, but unbiased stereology shows no significant loss of neurons in the amygdala or cortex. Fibril injected mice show defects in a social dominance behavioral task and fear conditioning, tasks that are associated with prefrontal cortex and amygdala function. Together, these observations suggest that seeded α-synuclein inclusion formation impairs behaviors associated with cortical and amygdala function, without causing cell loss, in brain areas that may play important roles in the complex cognitive features of PDD

* Corresponding author at: Center for Neurodegeneration and Experimental Therapeutics, University of Alabama at Birmingham, 1719 6th Avenue South, Birmingham, AL 35294, USA. lvolpicellidaley@uabmc.edu (L.A. Volpicelli-Daley).

Declaration of competing interest

None.

Appendix A. Supplementary data

Supplementary data to this article can be found online at https://doi.org/10.1016/j.nbd.2019.104708.

Keywords

Dementia with Lewy Bodies; Parkinson's disease dementia; Alpha-synuclein; Fear conditioning; Social dominance; Fibrils; Cortex; Amygdala; Lewy neurites; Lewy bodies; Excitatory neurons

1. Introduction

Parkinson disease (PD) is characterized by loss of dopaminergic neurons in the substantia nigra pars compacta (SNpc) and intracellular inclusions composed mostly of α-synuclein, called Lewy bodies and Lewy neurites. Symptoms classically include tremor, rigidity, bradykinesia, and postural instability (Kalia and Lang, 2015). In addition to the initial extrapyramidal motor effects, individuals living with PD can eventually develop cognitive changes and psychiatric disturbances such as depression and anxiety (Jellinger, 2018; Russell et al., 2014). Conversely, Dementia with Lewy Bodies (DLB) presents first with cognitive changes followed by development of parkinsonism. DLB and PD are considered within a spectrum of synucleinopathies, with both having a loss of dopamine terminals within the striatum as well as Lewy bodies and Lewy neurites found throughout the brain in regions important for cognition, such as the cortex, and limbic regions, including the amygdala (Adler and Beach, 2016; Braak et al., 1994; Braak et al., 2003). In addition, approximately 60% of Alzheimer's disease patients show Lewy pathology in the amygdala (Kotzbauer et al., 2001; Uchikado et al., 2006), suggesting that α-synuclein inclusions may contribute to behavioral changes associated with multiple neurodegenerative diseases. Supporting a role for α-synuclein in cognition and psychiatric symptoms are findings that severe dementia and psychiatric disturbances, such as fear and anxiety, predominate in patients with triplication of the SNCA gene, and in those with dominantly inherited mutations in SNCA, which supports a role for abnormal α-synuclein in these non-motor phenotypes (Lesage et al., 2013; Polymeropoulos et al., 1997; Singleton et al., 2003; Zarranz et al., 2004). A negative correlation between the density of α-synuclein pathology, particularly Lewy neurites, in the cortex and cognition also suggests a possible causal role of α-synuclein pathology and cognitive deficits (Beach et al., 2009; Irwin et al., 2017; Irwin and Hurtig, 2018; Irwin et al., 2013; Irwin et al., 2012). However, analyses of Lewy bodies in the cortex showed that some patients had Lewy bodies but did not receive a diagnosis of dementia (Colosimo et al., 2003; Parkkinen et al., 2005). Animal models of synucleinopathy could help us understand the contribution of abnormal aggregates of α-synuclein on behaviors related to cortical and limbic dysfunction. Although current treatments improve motor symptoms, treatments for cognitive symptoms show minimal effectiveness and no treatments are able to stop disease progression. Pathogenesis must be further explored, especially regarding the contribution of α-synuclein pathology on cognitive decline and behavioral disturbances.

The α-synuclein fibril model recapitulates many features of PDD and DLB. According to this model, exposure of neurons to small fragments of fibrillar α-synuclein generated from recombinant protein induces recruitment of endogenously expressed α-synuclein into inclusions. Similar to Lewy pathology found in individuals that suffered from PD and DLB, these inclusions are hyperphosphorylated, ubiquitinated, and filamentous (Volpicelli-Daley

et al., 2011). The inclusions form in the substantia nigra pars compacta (SNpc), causing loss of dopamine neurons and motor defects. In addition, similar to PD and DLB, inclusions are found in other brains regions, including the cortex and amygdala (Luk et al., 2012a). In vivo imaging, which allows imaging of the same neurons over several weeks to months, shows that neurons with inclusions generated from fibril exposure eventually die, demonstrating inclusions cause toxicity in these neurons (Osterberg et al., 2015). Furthermore, early formation of fibril-induced inclusions in excitatory neurons causes synaptic dysfunction demonstrating that α-synuclein aggregation causes neuronal dysfunction even before neuron death (Blumenstock et al., 2017; Froula et al., 2018; Wu, 2019). The effects of inclusions on neurons in the cortex and amygdala may lead to non-motor behavioral defects.

Here, we show that bilateral injections of fibrils into the striatum result in robust α-synuclein inclusion formation in the amygdala and in the cortex, primarily corticostriatal projection neurons in layers IV/V. Fibril injected mice show defects in a social dominance behavioral task associated with prefrontal cortex function. They also show defects in fear conditioning, which is associated with amygdala function. Multiple interconnected neural networks are responsible for cognitive function; while lesions of individual regions (such as the basolateral amygdala in fear conditioning or prefrontal cortex in social dominance) causes clear phenotypes, an interplay between these regions is likely the cause for phenotypes observed. Indeed, prefrontal cortical function (in addition to the amygdala) plays a role in contextual fear conditioning (Rozeske et al., 2015); similarly, amygdalar dysfunction has been implicated in social dominance (Phillips and LeDoux, 1992). Inclusions in the amygdala and prefrontal cortex primarily localized to excitatory neurons. Together, these observations suggest fibril exposure can be an important technique in studying the non-motor deficits of PD and DLB.

2. Materials and methods

Unless otherwise stated, all materials were purchased from Fisher Scientific.

2.1. Animals

All animal protocols were approved by the Institutional Animal Care and Use Committee at the University of Alabama at Birmingham. C57BL/6J mice were obtained from Jackson Labs. Mice were on a 12-h light/dark cycle and had ad libitum access to food and water. Both male and female mice were used in this study.

2.2. Preparation of fibrils

Mouse α-synuclein was purified in E. coli as described previously. A Pierce LAL high capacity endotoxin removal resin was used to minimize endotoxin (Volpicelli-Daley et al., 2014). Endotoxin levels were 0.017 Unit/μg of protein. The concentration of monomeric α-synuclein was measured by absorbance at 280 nm with an extinction coefficient of 7450 M^{-1} cm^{-1}. Fibrils were generated by incubating monomeric α-synuclein (300 μM) in 150 mM KCl, 50 mM Tris-HCl at 37 °C with constant agitation for 7 days (Bousset et al., 2013). After the seventh day, fibrils were isolated from remaining monomer by centrifugation for 10 min at 13,200 rpm and resuspended in half the initial volume of buffer. Five μL of fibrils

were incubated for 1 h with 8 M guanidinium chloride to dissociate the fibrils into monomer, the concentration of α-synuclein was measured, and remaining fibrils were diluted to a final concentration of 300 μM. On the day of injection, fibrils were sonicated using a probe tip sonicator (Fisher, FB120110) for 30 s total time, with 1 s pulses at 30% amplitude.

2.3. Intrastriatal injection of recombinant α-synuclein fibrils

At 3 to 4 months of age, male and female mice were deeply anesthetized with vaporized isoflurane on a stereotactic frame. Animals were bilaterally injected with 2 μL (per side) of 300 μM sonicated fibrils, or 300 μM monomeric α-synuclein, or phosphate-buffered saline (PBS) as controls. Solutions were injected at a constant rate of 0.5 μL/ min and the needle left in place for 5 min followed by slowly withdrawing the needle. Coordinates for the striatum were + 0.2 mm AP, ± 2.0 mm ML, −2.6 mm DV. Two separate cohorts were utilized in this study. The first cohort had an experimental group injected with sonicated fibrils and a control group injected with PBS, as performed previously (Luk et al., 2012a). However, recent evidence has suggested monomeric α-synuclein as a control for injection of α-syn protein is the optimal control (Polinski et al., 2018). Therefore, a second cohort using monomeric α-synuclein was used for tube test analyses. No differences were noted between the experimental groups.

2.4. Behavior testing

Behavior tests to assess motor and non-motor function were conducted 6 months after injection of fibrils or control. Mice were handled for 3 days before testing began and habituated to testing room for 1 h at the start of each testing day. The order of test was designed to minimize stress to the animals, such that low-stress tasks were completed before high-stress tasks. Additionally, mice received at least one rest day between each test. Specifically, mice completed behavior testing in the order listed below, with the first cohort completing open field, elevated zero maze, rotarod, and fear conditioning. The second cohort also completed open field test followed by tube test. The researcher conducting the tests was blinded to treatment. To minimize scents, all apparatuses were cleaned with 70% ethanol between trials.

2.5. Open field test

To test general motor activity as well as anxiety, mice were placed in a clear plastic chamber, and allowed to explore for 10 min. Noldus Ethovision XT 11 recorded the total distance traveled, as well as time spent in center of the chamber.

2.6. Elevated zero maze

To test anxiety, mice underwent a variant of the elevated plus maze. In this variant, mice are placed in an elevated maze consisting of a single, round track. Half of the track is enclosed, with quarters of the track being divided (Kulkarni et al., 2007; Tucker and McCabe, 2017). Mice were placed at a uniform starting location at the border between an open and enclosed arm and allowed to freely explore for 5 min. Total time spent in open and closed arms was recorded.

2.7. Rotarod

To further test motor activity, mice were placed on an accelerating rotarod apparatus, and time taken to fall was measured. Mice were trained on the apparatus over 5 days, with the rotarod speed increasing from 4 rpm to 40 rpm over 300 s. If mice had not fallen by 120 s on the testing trial, the rotation was halted, the mouse was removed, and the time was recorded as 120 s. Mice underwent two trials per day, with an inter-trial rest time of at least 30 min.

2.8. Cued and contextual fear conditioning

To test fear learning and memory, mice were placed in a novel environment and trained to associate a tone (conditioned stimulus; CS) with a mild foot shock (unconditioned stimulus, US). After 2 min in the novel environment, a continuous tone would play for 30 s, culminating with a mild (0.8 mA) foot shock that lasted 2 s. One minute later, the tone and shock would repeat. Mice showed a fear response by exhibiting freezing behavior. During testing, mice were placed in the same environment for 5 min and freezing behavior was measured for every minute. One hour later, mice were exposed to a novel environment and the US is re-presented, this time without the foot shock. Freezing behavior during the tone was measured. Freeze Frame software was used to record sessions, and freezing behavior was scored by an experimenter blinded to conditions. Freezing behavior was defined as previous (Blanchard and Blanchard, 1969; Fanselow, 1990; Paylor et al., 1994) as the absence of movement except for respiratory-related movements.

2.9. Tube test

Tubing was uniformly 30.5 cm long, but a range of internal diameters (ID) were used based on animal size to dissuade mice from climbing over each other, requiring them to push the other out of the tube to proceed forward. Mice were paired with a non-cagemate mouse of the same sex and released into opposite ends of a tube. As previously published, all mice (monomer and fibril injected) were prompted to enter the tube and were not released until both mice had all four paws within the tube (Arrant et al., 2016). Mice were tested against a total of 3 other animals and side of the tube was randomly chosen. The first mouse with two feet outside of the tube was considered non-dominant. Any test that lasted longer than 2 min was aborted and re-run at the end of the testing cycle.

2.10. Immunofluorescence and immunohistochemistry

At 3 or 6 months after injection, after the completion of behavior testing, mice were deeply anesthetized with isoflurane and transcardially perfused with 0.9% saline and 10 units/mL heparin and sodium nitroprusside (0.5% w/v) followed by cold 4% paraformaldehyde (PFA) in phosphate buffered saline (PBS). Brains were dissected, postfixed in 4% PFA in PBS for 12 h at 4 °C, cryoprotected with 30% sucrose in PBS for 24–48 h, and stored at −80 °C. Brains were sectioned at 40um thickness on a freezing microtome and stored in 50% glycerol, 0.01% sodium azide in tris-buffered saline (TBS). Serial sectioning was performed by placing each section into a well of a 6 well tray such that one well represented the entire forebrain with sections spaced 240 μm apart. For immunofluorescence, sections were rinsed five times in TBS and then incubated in an antigen retrieval solution (10 mM sodium citrate, 0.05% Tween-20, pH 6.0) for 1 h at 37 °C. Sections were blocked and permeabilized for 1

h at 4 °C with agitation in 5% normal goat or donkey serum, 0.01% TritonX-100 in TBS. Next, sections were rinsed and then incubated in primary antibody in 5% normal goat or donkey serum (Equitech-Bio Inc) in TBS for 24 h at 4 °C with agitation. Table 1 shows the primary antibodies used. The pSer-129-α-syn antibodies have been extensively used elsewhere and validated using tissue from α-synuclein knockout mice (Delic et al., 2018; Rutherford et al., 2016). After rinses, sections were incubated with secondary antibodies (Goat anti-mouse IgG1 Alexa Fluor 488 conjugate, Goat anti-mouse IgG2a Alexa Fluor 555 conjugate, or Goat anti-rabbit IgG Alexa Fluor 555; Invitrogen) in 5% goat or donkey serum in TBS for 2 h at 4 °C with agitation. Sections were then rinsed and mounted on charged slides using Prolong Gold (Invitrogen). Brains from animals sacrificed 3 months after injection were utilized to identify pSer29-α-synuclein inclusions, as we and others have reported a peak in inclusion burden at 2–3 months post-injection (Patterson et al., 2019). It has been suggested that these inclusions eventually disappear, likely as the neurons die off, but potential clearance of aggregates remains to be rigorously tested (Osterberg et al., 2015). All other tests and analyses (including unbiased stereologic counts) used brains from animals sacrificed 6 months after injection.

For immunohistochemistry, sections were rinsed five times in TBS and then quenched in 0.6% H_2O_2 in TBS for 20 min, followed by rinsing. Sections then underwent antigen retrieval, blocking, and primary antibody solutions as above. Biotin-SP AffiniPure Donkey Anti-Mouse IgG H&L (Jackson ImmunoResearch) was used as a secondary antibody; sections were then incubated with Avidin-Biotin Complex Peroxidase Standard Staining Kit reagent for 30 min at 4 °C and then developed using ImmPACT-3, 3′-diaminobenzidine (DAB, Vector Labs). Sections were sequentially dehydrated using ethanol and Histo-Clear (30 s water followed by 3 min each 70%, 95%, 95%, 100%, and 100% ethanol, culminating in three 5 min washes in Histo-Clear) and mounted on charged slides using Permount.
For proteinase K digestion, sections were incubated in 20 μg/mL proteinase K diluted in in tris-buffered saline for 10 min at 37 °C. Following 3 rinses in TBS, sections were incubated in 0.6% H_2O_2 for 20 min, rinsed, blocked with 5% normal goat serum, and 0.05% Tx-100 for 30 min, and then incubated with an antibody to total α-synuclein overnight (Abcam AB51252) at 4 °C in TBS/5% normal goat serum. The sections were then incubated biotinylated goat anti-rabbit secondary antibody (Jackson Immunoresearch), followed by avidin-biotin complex (Vector Labs), and developed using ImmPACT-3,3′-diaminobenzidine substrate kit (Vector Labs).

2.11. Fluorescent microscopy, colocalization quantitation, and unbiased stereology

Sections were imaged using a Zeiss Axiovert.Z1 microscope for wide-field fluorescence, Olympus BX51 microscope for bright field, or a Leica TCS-SP5 laser scanning confocal microscope. The researcher capturing images was blinded to the treatment group. At least 3 images were obtained from each region of interest for analysis. Colocalization was then determined using the JACoP plugin from ImageJ (Bolte and Cordelieres, 2006).

Unbiased stereological analyses were conducted on a brightfield microscope using an optical fractionator probe (Stereo Investigator software, Stereology Resource Center) on sections immunoprocessed for NeuN and were conducted by a researcher blinded to the

experiment. For stereology of the basolateral amygdala, a 4× objective was used to identify the borders (see Fig. 5B). Sections covered the entire BLA amygdala and were equally spaced 200um apart. Ten percent of the area was quantified, with a guard zone height of 2um to avoid artifacts. A total of 6–8 sections per animal were quantified. Stereology of the prefrontal cortex was modeled based on a previous study (Lemmens et al., 2011), and serial sectioning was used to identify sections between bregma coordinates +2.46 to +1.10 mm. The prefrontal cortex was delineated using a 4× objective. The optical dissector height was 22 μm and the distance between the counting frame was 250 by 250 μm. The counting variability was measured with the Schmitz-Hof coefficient of error (CE) (Schmitz, 1998) and was 0.017.

2.12. Statistical analyses

Analyses and graphs were generated using GraphPad Prism. Significance between groups for the fear acquisition tests was determined by repeated measures analysis of variance (ANOVA). Open field, elevated zero maze, fear conditioning, and stereology used unpaired t-tests. A binomial test was used for tube test. An ANOVA was utilized for determining significance in colocalization analyses. All data fit a normal distrubtion as determined by a Shapiro-Wilk or Kolomogorov-Smirnov test for normality.

3. Results

3.1. Localization of α-synuclein inclusions in cortex and amygdala following bilateral intrastriatal injections of fibrils

Mice received bilateral injections into the dorsolateral striatum with α-synuclein fibrils or controls. To examine the localization of α-synuclein inclusions, immunofluorescence was performed using an antibody that recognizes α-synuclein phosphorylated at Ser129 (pSer129-α-syn). This antibody recognizes Lewy neurites and Lewy bodies in PD and DLB brains (Fujiwara et al., 2002). In rodents, exposure of neurons to fibrils induces formation of p-α-synuclein inclusions (Ayers et al., 2017; Luk et al., 2012a; Masuda-Suzukake et al., 2014; Osterberg et al., 2015; Paumier et al., 2015; Rey et al., 2018; Sacino et al., 2013). However, there is very little pSer129-α-synuclein in neurons from wild type mice injected with PBS or monomer, or fibril exposed neurons from α-synuclein knockout mice (Delic et al., 2018; Dhillon et al., 2017; Volpicelli-Daley et al., 2011) (Also see supplemental fig. 1, this study). Here, bilateral injections of fibrils produced pSer129-α-synuclein positive inclusions in the amygdala (Fig. 1A), which projects to the striatum (Hunnicutt et al., 2016). Both the central and basolateral amygdala showed thread-like pSer129-α-synuclein positive inclusions that appeared similar to Lewy neurites, and skein-like inclusions in the soma in the amygdala (Fig. 1B). Double labeling immunofluorescence with pSer129-α-synuclein and the neuron specific marker, NeuN, confirmed that the somal inclusions were found in neurons (Fig. 1B).

Abundant pSer129-α-synuclein inclusions were also found in the cortex (Fig. 2A); in particular, the following areas of the cortex showed pSer129-α-synuclein inclusions: prefrontal, prelimbic, somatosensory, motor, cingulate, insular, perirhinal, and entorhinal (Fig. 2A). Layers IV/V and VI of the cortex, which contain corticostriatal projection

neurons, particularly showed a robust burden of pathologic α-synuclein (Fig. 2B, C), and a distinct “band” of pSer129-α-synuclein positive inclusions appeared throughout many cortical regions (see Fig. 2A). Similar to the amygdala, the majority of inclusions in the soma appeared juxtaposed to NeuN, demonstrating localization to neurons (Fig. 2B). To confirm that these inclusions localized to layer IV/V, double labeling immunofluorescence was performed with antibodies to pSer129-α-synuclein and Necab1, a calcium signaling molecule with selective expression in layer IV/V cortical neurons (Fig. 2C; Sugita et al., 2002). The majority of pSer129-α-synuclein inclusions showed overlap with Necab1 in layers IV/V. As another method to visualize α-synuclein inclusions, immunohistochemistry was performed on tissue sections treated with proteinase K, which digests normal α-synuclein, and incubated in an antibody that recognizes total α-synuclein (Supplemental Fig. 2). The proteinase K aggregates appeared very similar in morphology as the pSer129-α-synuclein inclusions. This method identified proteinase K insoluble α-synuclein as another way to identify inclusions independent of the pSer129-α-synuclein. In the cortex and amygdala of proteinase K treated sections from control injected mice, there are no aggregates of α-synuclein. In the cortex and amygdala of fibril injected mice, proteinase K resistant α-synuclein aggregates are visible in the soma and in neurites (Supplemental fig. 2).

In accordance with other studies (Abdelmotilib et al., 2017; Luk et al., 2012a), pSer129-α-synuclein inclusions were seen in the substantia nigra pars compacta and striatum following injection with fibrils (Supplemental fig. 3). Studies completed by others and within our lab have shown a 20–30% loss of TH+ neurons in the substantia nigra at 6 months after fibril injection (Froula et al., 2019).

3.2. Fibril-injected mice show impaired fear memory and social dominance

Behavioral assays of motor, cortical, or amygdala function were performed to determine the extent of behavioral phenotypes. Compared to controls, fibril-injected mice showed no significant deficits on gross motor function or anxiogenic behavior as evaluated by open field test (Fig. 3A–C). There were no significant differences between control mice and mice injected with fibrils in the total distance traveled (Fig. 3A), time spent in the center of the field (Fig. 3B), or velocities of movement (Fig. 3C). Additionally, there was no effect on time to fall in the accelerating rotarod test for motor dysfunction when comparing fibril to PBS (Fig. 3D). Overall, mice did not exhibit overt motor defects, suggesting there would be no confounding factor of reduced motor function on further behavioral tests of cortical and amygdala function.

Mice exhibited robust inclusions in the basolateral amygdala after intrastriatal fibril injections (Fig. 1B), suggesting an amygdala-dependent phenotype may be present at later time points. To test this, mice underwent tests for anxiety, and fear learning and memory. For the acquisition phase of fear learning, mice were subject to two foot shocks introduced at the culmination of a 30 s auditory tone. Fibril-injected mice did not significantly differ from control animals during the acquisition phase of fear conditioning (Fig. 4A). As expected, mice increased in freezing behavior from pre-shock to post-shock behavior. Freezing behavior was comparable between groups before administration of the first unconditioned

stimulus (foot shock), and increased in both groups up to 80% after both foot shocks had been administered. For cued fear conditioning, mice were exposed to a novel environment and allowed to briefly explore before being re-introduced to the auditory tone from fear acquisition. Freezing behavior for the duration of the tone was measured. Fibril-injected mice and control mice showed no difference in cued fear conditioning (Fig. 4B). During contextual fear conditioning, mice were exposed to the same context (cage) as during fear acquisition, and freezing behavior for the duration of exposure was measured. Compared to control mice, mice that received bilateral injections of fibrils showed a significant decrease of approximately 20% in percent time freezing during the first minute of exposure in contextual fear conditioning (Fig. 4C). This suggests fibril-injected mice were specifically impaired in contextual fear conditioning.

We further tested anxiety behavior via the elevated zero maze, a variant of the elevated plus maze, which utilizes thigmotaxic behavior to evaluate anxiety and amygdala function. According to this test, increased anxiety is indicated by an increase in the proportion of time spent in closed arms. In this study, mice spent the majority of time in the closed arms, and there were no significant differences in the percentage of time spent in the closed arms between fibril-injected mice compared to control animals (Fig. 4D–E). These data suggest that fibril-injected mice had no impairment in innate anxiety-specific behavior.

Given the abundant pSer129-α-synuclein inclusions in the cortex, we performed behavioral tests of cortical function. The social dominance test reveals defects in prefrontal cortical function (Arrant et al., 2016; Filiano et al., 2013; Lindzey et al., 1961; Wang et al., 2014). In the experiments performed in this study, non-cagemates were placed in a clear tube as one pushed the other, less dominant mouse, out of the tube (Fig. 4F). When a mouse had two hind paws outside the tube, it was scored a 0, for non-dominant and the other mouse was scored a 1, for dominant. Fibril-injected mice were less socially dominant than control mice across trials (Fig. 4G), with the cohort winning less than a third of all runs. The majority of control animals won at least 2 of their 3 trials (Fig. 4H), which showed a significant difference in wins per mouse. This suggests that fibril-injected mice are less socially-dominant than control mice.

3.3. Basolateral amygdala inclusions are selectively found in excitatory neurons

Unilateral fibril injections cause an approximately 30% loss of tyrosine-hydroxylase positive neuron loss in the ipsilateral SNpc (Luk et al., 2012b). However, it is unknown if other brain regions show similar degeneration. To assess if the inclusions in the basolateral amygdala (Fig. 5A) led to neurodegeneration at 6 months, we performed immunohistochemistry for the neuron selective marker, NeuN, and unbiased stereology to count neurons. The basolateral amygdala was identified as the region of interest (Fig. 5B) and serial sections were quantified. Stereologic counts revealed an approximately 13% loss of volume, and a 18% loss of neurons in fibril injected mice compared to controls measured by volumetric and cell counts, respectively, in the experimental animals compared to controls (Fig. 5C). However, the differences between the two groups did not achieve significance ($p < .055$). Correlation between stereologic estimates (Fig. 5C) and context-specific freezing behavior

(Fig. 4C) failed to show significance (Supplemental fig. 4), suggesting that neuron loss alone may not be the only effector on behavioral outcomes.

To determine the neuronal subtype to which α-synuclein localizes in the amygdala, double labeling immunofluorescence for pSer129-α-synuclein and CaMKII, or SATB2, markers of excitatory neurons (Bemben et al., 2014; Huang et al., 2013), or parvalbumin, calretinin, and calbindin, markers of inhibitory neurons. In the amygdala, pSer129-α-synuclein-positive inclusions were localized almost exclusively to excitatory neurons (Fig. 5D). Specifically, SATB2+ cells extensively colocalized with pSer129-α-synuclein. Quantitation of colocalization revealed an 89% overlap with SATB2+. pSer129-α-Synuclein inclusions also overlapped with the excitatory neuron marker, CamKII+, although to a slightly lesser extent than SATB2+, with a 63% overlap. In contrast, pSer129-α-synuclein showed minimal overlap with the inhibitory neuron markers, parvalbumin, calretinin, and calbindin-positive neurons, with a 1.2, 0.9, and 3.5% overlap, respectively (Fig. 5E).

3.4. Prefrontal cortical inclusions are specific to excitatory neurons

Stereologic analyses allowed for evaluation of potential neurodegeneration in the prefrontal cortex. Estimations revealed no significant difference in NeuN+ cell count or volume of the prefrontal cortex, with both groups containing approximately 1 million neurons (Fig. 6B and C). This suggests that neuron loss alone cannot be responsible for behavioral dysfunction, and inclusions are likely leading to cellular dysfunction before cell death (Froula et al., 2018). However, it cannot be excluded that a more detailed evaluation of specific cell layers or regions within the prefrontal cortex may reveal specific degeneration.

Similar to the basolateral amygdala, a high percentage of excitatory neurons contained pSer129-α-synuclein-positive inclusions in the prefrontal cortex (Fig. 6A). Specifically, SATB2+ and CamKII+ neurons colocalized extensively with pSer129-α-synuclein in the prefrontal cortex, with SATB2+ overlapped at 100% and CamKII+ at a 55% overlap. Triple immunofluorescence imaging with pSer129-α-synuclein, CamKII, and SATB2 showed that in both the amygdala and prefrontal cortex, CAMKII overlaps with SATB2, however there exist SATB2 neurons with no immunofluorescence for CAMKII, which could account for a higher proportion of pSer129-α-synuclein inclusions colocalizing with SATB2 (Supplemental fig. 5). Markers of inhibitory neurons (parvalbumin, calretinin, and calbindin) did not colocalize with inclusions (Fig. 6B), with an overlap of 1.9%, 2.2%, and 10.8%, respectively. Therefore, the majority of α-synuclein inclusions in the amygdala and cortex localized to excitatory neurons.

4. Discussion

It has been previously shown that unilateral injection of fibrils into the striatum induce formation of inclusions located in the SNpc, among other brain regions, (Abdelmotilib et al., 2017; Luk et al., 2012a; Masuda-Suzukake et al., 2013). Most of these studies focus on the effect of seeded α-synuclein inclusion formation on loss of dopamine neurons in the SNpc because reduced nigral-striatal dopamine is responsible for motor deficits in PD. However, little is known about the impact of abnormal α-synuclein in other brain regions, other neuron subtypes, and the potential consequence for the non-motor phenotypes

related to PDD and DLB. This is important because α-synuclein inclusions, and amygdala and cortical changes, are well documented in PDD/DLB patients, and likely contribute to cognitive changes and psychiatric disturbances (Beach et al., 2009; Bowers et al., 2006; Halliday et al., 2014; Hurtig et al., 2000; Irwin et al., 2013; Kempster et al., 2010; Mattila et al., 2000; Trnka et al., 2018). In this study, bilateral injections of fibrils into the mouse striatum produced robust pathology in the central and basolateral amygdala on both sides of the brain, as well as throughout the neocortex, particularly in layers IV/V. These inclusions were pSer129 positive and resistant to proteinase K digestion. The brain regions identified send projections to the dorsolateral striatum (Hunnicutt et al., 2016). A potential avenue for further research would be to determine if injection directly into the prefrontal cortex or amygdala would produce similar results, or if retrograde transport of misfolded α-synuclein is necessary for dysfunction. The inclusions appeared predominantly in excitatory neurons, consistent with enrichment of α-synuclein in this neuronal subtype (Taguchi et al., 2016). Mice with inclusions showed reduced performance in fear conditioning, a measure of amygdala function, and the social dominance test, a measure of prefrontal cortex function. Thus, our findings suggest that bilateral injections of fibrils into the striatum provides a model of cortical and amygdala dysfunction in PDD and DLB.

Our data support other studies showing cognitive impairments in other mouse models of synucleinopathy. In particular, overexpression of human α-synuclein using the Thy1 promoter produces cognitive and behavioral phenotypes (Chesselet et al., 2012; Magen et al., 2012; Magen et al., 2015). These mice presented with difficulties in rule-reversing tests, spontaneous alternation, and an increase in anxiety. Thus, our data contribute to the growing evidence that abnormal α-synuclein contributes to non-motor phenotypes in PDD and DLB. One advantage of the fibril model is that endogenously expressed α-synuclein is corrupted. This feature allows researchers to assess which neurons are particularly vulnerable to α-synuclein aggregation without the potential confound of aberrant α-synuclein expression caused by the Thy1 promoter.

α-Synuclein normally localizes to the presynaptic terminal and axons (Boassa et al., 2013; Vargas et al., 2017). In this study, we showed that intrastriatal fibril injections produced abundant inclusions in brain nuclei that project to the striatum. This supports the previous in vitro finding of aggregates initially forming in axons and retrogradely traveling to the soma (Bieri et al., 2018; Brahic et al., 2016; Volpicelli-Daley et al., 2011). In addition, fibril-induced inclusions predominantly formed in neurons in which α-synuclein is highly expressed, particularly glutamatergic excitatory neurons (Taguchi et al., 2016). Inhibitory neurons in the cortex and amygdala expressing calretinin, calbindin, or parvalbumin showed minimal to no inclusion formation, similar to findings in brains from patients who suffered from PD and DLB (Gomez-Tortosa et al., 2001). This suggests that susceptibility to forming α-synuclein inclusions is dependent on cell type (excitatory vs. inhibitory), endogenous α-synuclein expression, and anatomical connections. It is also possible that the higher expression of calcium buffering proteins in inhibitory neurons prevented calcium activated protease cleavage of α-synuclein, which enhances fibrillization (Duftyet al., 2007). In addition, it is also possible that excitatory neurons express lower levels of proteins involved in degradative pathways, thus leading to buildup of aggregates, as has been shown for the tau protein (Fu et al., 2019).

Fibril-injected mice show abundant inclusions in the amygdala and defects in fear conditioning. Fear conditioning in mice is partially an amygdala dependent test, suggesting that fibril injections and α-synuclein inclusions caused dysfunction in this brain region (Ciocchi et al., 2010; Muller et al., 1997; Phillips and LeDoux, 1992; Rozeske et al., 2015). However, the fibril injected mice did not show significant differences in the elevated plus maze or the open field test, also tests of amygdala function and anxiety. It is possible that the fibril injected mice had a selective defect in conditioned fear memory as revealed by the contextual fear conditioning, but not in innate, unconditioned fear responses such as walking in the open arms in a raised platform. Also, the α-synuclein inclusions also apspeared in other brain areas such as the prefrontal cortex and midbrain dopamine neurons, which also play a role in fear memory (Curzon et al., 2009; Rozeske et al., 2015). Thus, complex defects in neuronal circuitry likely contributed to the differences in the distinct behavioral tasks.

The tube test for social dominance has been shown to be functionally dependent on the prefrontal cortex (Arrant et al., 2016; Filiano et al., 2013; Wang et al., 2011) and amygdala (Jonason and Enloe, 1971) in rodent models, with both dysfunction and lesions impairing performance. Thus, fibril-injected mice likely showed defects in the tube test resulting from neuronal dysfunction in the prefrontal cortex and/or amygdala. This behavior translates to humans, as the prefrontal cortex also plays a role in social hierarchies, working memory, attention, and inhibition control (Schneider and Koenigs, 2017; Teffer and Semendeferi, 2012) – all functions that are impaired in PD or DLB (Jellinger, 2012). Therefore, we believe these phenotypes produced by bilateral intrastriatal injections represented a model of non-motor manifestations of synucleinopathies.

Overall, bilateral injection of synuclein fibrils cause defects in fear conditioning and social dominance which may provide a model of dysfunction in the cortex and amygdala, helping us to further understand mechanisms that contribute to some of the cognitive phenotypes in PDD and DLB. These symptoms are associated with inclusions reminiscent of Lewy body pathology in both regional and cellular location, as well as subcellular morphology and modifications. Specifically, pSer129-α-synuclein positive and protease K resistant inclusion burden was heavy in amygdala and prefrontal cortex, both areas shown to correlate with cognitive dysfunction and psychiatric symptoms in synucleinopathy patients (Beach et al., 2009; Bowers et al., 2006; Halliday et al., 2014; Hurtig et al., 2000; Irwin et al., 2013; Kempster et al., 2010; Mattila et al., 2000; Trnka et al., 2018). The observations noted in this manuscript support the hypothesis that inclusions of α-synuclein contribute to symptoms observed in PDD and DLB. It is important to note however, that other pathologies likely contribute to cognitive changes as well including concomitant AD-like pathology, and/or cerebrovascular lesions which should be studied in the future. Non-motor and cognitive symptoms remain largely untreated in PDD/DLB patients, with therapies such as acetylcholinesterase inhibitors providing only mild to moderate relief of symptoms (Kalia and Lang, 2015). Cognitive and behavioral impairments are the biggest reason for institutionalization and lead to rapid decline of patient quality of life. Thus, these findings provide an avenue for elucidating mechanistic causes to sporadic synucleinopathies and determining potential therapeutics for halting cognitive decline in synucleinopathy patients.

Supplementary Material

Refer to Web version on PubMed Central for supplementary material.

Acknowledgements

We would like to thank Dr. Erik Roberson for his advice and expertise related to the project. We would like to thank Anner Harris for performing the SATB2/CAMKII/pSer129-α-synuclein triple immunofluorescence. We thank Dr. Van Groen for his expertise in the behavioral tasks and the UAB Behavioral Assessment Core P30 NS47466. Funding support was from the Department of Defense Parkinson's Research Program Award number PD150032 to L.V.-D., NIH F30 AG058458, NIH R01 NS102257 to L.V.D. and P50NS108675 (Alabama Udall Center) to D.G.S.

Abbreviations

α-synuclein	alpha-synuclein
AAV	adeno-associated virus
ANOVA	analysis of variance
BLA	basolateral amygdala
CamKII	Ca2+/calmodulin-dependent protein kinase II
CS	conditioned stimulus
DAB	3,3′-diaminobenzidine
DLB	Dementia with Lewy Bodies
ID	internal diameters
LB	Lewy body
MMSE	mini-mental state examination
Necab1	N-terminal EF-hand calcium binding protein 1
NeuN	neuronal nuclei
p- α-synuclein	alpha-synuclein phosphorylated at Ser129
PBS	phosphate-buffered saline
PD	Parkinson's disease
PDD	Parkinson's disease dementia
PFA	paraformaldehyde
PV	parvalbumin
REM	rapid eye movement
SATB2	special AT-rich sequence-binding protein 2
SNpc	substantia nigra pars compacta

TBS	tris-buffered saline
US	unconditioned stimulus

References

Abdelmotilib H, et al. , 2017. alpha-Synuclein fibril-induced inclusion spread in rats and mice correlates with dopaminergic neurodegeneration. Neurobiol. Dis 105, 84–98. [PubMed: 28576704]

Adler CH, Beach TG, 2016. Neuropathological basis of nonmotor manifestations of Parkinson‘s disease. Mov. Disord 31, 1114–1119. [PubMed: 27030013]

Arrant AE, et al. , 2016. Progranulin haploinsufficiency causes biphasic social dominance abnormalities in the tube test. Genes Brain Behav. 15, 588–603. [PubMed: 27213486]

Ayers JI, et al. , 2017. Robust central nervous system pathology in transgenic mice following peripheral injection of alpha-Synuclein fibrils. J. Virol 91.

Beach TG, et al. , 2009. Unified staging system for Lewy body disorders: correlation with nigrostriatal degeneration, cognitive impairment and motor dysfunction. Acta Neuropathol. 117, 613–634. [PubMed: 19399512]

Bemben MA, et al. , 2014. CaMKII phosphorylation of neuroligin-1 regulates excitatory synapses. Nat. Neurosci 17, 56–64. [PubMed: 24336150]

Bieri G, et al. , 2018. Internalization, axonal transport and release of fibrillar forms of alpha-synuclein. Neurobiol. Dis 109, 219–225. [PubMed: 28323023]

Blanchard RJ, Blanchard DC, 1969. Crouching as an index of fear. J. Comp. Physiol. Psychol 67, 370–375. [PubMed: 5787388]

Blumenstock S, et al. , 2017. Seeding and transgenic overexpression of alpha-synuclein triggers dendritic spine pathology in the neocortex. EMBO Mol. Med 9, 716–731. [PubMed: 28351932]

Boassa D, et al. , 2013. Mapping the subcellular distribution of alpha-synuclein in neurons using genetically encoded probes for correlated light and electron microscopy: implications for Parkinson‘s disease pathogenesis. J. Neurosci 33, 2605–2615. [PubMed: 23392688]

Bolte S, Cordelieres FP, 2006. A guided tour into subcellular colocalization analysis in light microscopy. J. Microsc 224, 213–232. [PubMed: 17210054]

Bousset L, et al. , 2013. Structural and functional characterization of two alpha-synuclein strains. Nat. Commun 4, 2575. [PubMed: 24108358]

Bowers D, et al. , 2006. Startling facts about emotion in Parkinson‘s disease: blunted reactivity to aversive stimuli. Brain 129, 3356–3365. [PubMed: 17095520]

Braak H, et al. , 1994. Amygdala pathology in Parkinson’s disease. Acta Neuropathol. 88, 493–500. [PubMed: 7879596]

Braak H, et al. , 2003. Staging of brain pathology related to sporadic Parkinson‘s disease. Neurobiol. Aging 24, 197–211. [PubMed: 12498954]

Brahic M, et al. , 2016. Axonal transport and secretion of fibrillar forms of alpha-synuclein, Abeta42 peptide and HTTExon 1. Acta Neuropathol. 131, 539–548. [PubMed: 26820848]

Chesselet MF, et al. , 2012. A progressive mouse model of Parkinson‘s disease: the Thy1aSyn (“Line 61”) mice. Neurotherapeutics 9, 297–314. [PubMed: 22350713]

Ciocchi S, et al. , 2010. Encoding of conditioned fear in central amygdala inhibitory circuits. Nature 468, 277–282. [PubMed: 21068837]

Colosimo C, et al. , 2003. Lewy body cortical involvement may not always predict dementia in Parkinson‘s disease. J. Neurol. Neurosurg. Psychiatry 74, 852–856. [PubMed: 12810766]

Curzon P, et al., 2009. Cued and contextual fear conditioning for rodents. In: Buccafusco JJ (Ed.), Methods of Behavior Analysis in Neuroscience. CRC Press/Taylor & Francis, Boca Raton (FL).

Delic V, et al. , 2018. Sensitivity and specificity of phospho-Ser129 alpha-synuclein monoclonal antibodies. J. Comp. Neurol 526, 1978–1990. [PubMed: 29888794]

Dhillon JS, et al. , 2017. A novel panel of alpha-synuclein antibodies reveal distinctive staining profiles in synucleinopathies. PLoS One 12, e0184731. [PubMed: 28910367]

Dufty BM, et al. , 2007. Calpain-cleavage of alpha-synuclein: connecting proteolytic processing to disease-linked aggregation. Am. J. Pathol 170, 1725–1738. [PubMed: 17456777]

Fanselow MS, 1990. Factors governing one-trial contextual conditioning. Anim. Learn. Behav 18, 264–270.

Filiano AJ, et al. , 2013. Dissociation of frontotemporal dementia-related deficits and neuroinflammation in progranulin haploinsufficient mice. J. Neurosci 33, 5352–5361. [PubMed: 23516300]

Froula JM, et al. , 2018. alpha-Synuclein fibril-induced paradoxical structural and functional defects in hippocampal neurons. Acta Neuropathol. Commun 6, 35. [PubMed: 29716652]

Froula JM, et al. , 2019. Defining α-synuclein species responsible for Parkinson‘s disease phenotypes in mice. J. Biol. Chem 294, 10392–10406. [PubMed: 31142553]

Fu H, et al. , 2019. A tau homeostasis signature is linked with the cellular and regional vulnerability of excitatory neurons to tau pathology. Nat. Neurosci 22, 47–56. [PubMed: 30559469]

Fujiwara H, et al. , 2002. alpha-Synuclein is phosphorylated in synucleinopathy lesions. Nat. Cell Biol 4, 160–164. [PubMed: 11813001]

Gomez-Tortosa E, et al. , 2001. Cortical neurons expressing calcium binding proteins are spared in dementia with Lewy bodies. Acta Neuropathol. 101, 36–42. [PubMed: 11194939]

Halliday GM, et al. , 2014. The neurobiological basis of cognitive impairment in Parkinson‘s disease. Mov. Disord 29, 634–650. [PubMed: 24757112]

Huang Y, et al. , 2013. Expression of transcription factor Satb2 in adult mouse brain. Anat. Rec. (Hoboken) 296, 452–461. [PubMed: 23386513]

Hunnicutt BJ, et al. , 2016. A comprehensive excitatory input map of the striatum reveals novel functional organization. Elife 5.

Hurtig HI, et al. , 2000. Alpha-synuclein cortical Lewy bodies correlate with dementia in Parkinson‘s disease. Neurology 54, 1916–1921. [PubMed: 10822429]

Irwin DJ, Hurtig HI, 2018. The contribution of Tau, amyloid-beta and alpha-synuclein pathology to dementia in Lewy body disorders. J. Alzheimers Dis. Parkinsonism 8.

Irwin DJ, et al. , 2012. Neuropathologic substrates of Parkinson disease dementia. Ann. Neurol 72, 587–598. [PubMed: 23037886]

Irwin DJ, et al. , 2013. Parkinson‘s disease dementia: convergence of alpha-synuclein, tau and amyloid-beta pathologies. Nat. Rev. Neurosci 14, 626–636. [PubMed: 23900411]

Irwin DJ, et al. , 2017. Neuropathological and genetic correlates of survival and dementia onset in synucleinopathies: a retrospective analysis. Lancet Neurol. 16, 55–65. [PubMed: 27979356]

Jellinger KA, 2012. Neurobiology of cognitive impairment in Parkinson‘s disease. Expert. Rev. Neurother 12, 1451–1466. [PubMed: 23237352]

Jellinger KA, 2018. Dementia with Lewy bodies and Parkinson‘s disease-dementia: current concepts and controversies. J. Neural Transm. (Vienna) 125, 615–650. [PubMed: 29222591]

Jonason KR, Enloe LJ, 1971. Alterations in social behavior following septal and amygdaloid lesions in the rat. J. Comp. Physiol. Psychol 75, 286–301. [PubMed: 5087378]

Kalia LV, Lang AE, 2015. Parkinson‘s disease. Lancet 386, 896–912. [PubMed: 25904081]

Kempster PA, et al. , 2010. Relationships between age and late progression of Parkinson‘s disease: a clinico-pathological study. Brain 133, 1755–1762. [PubMed: 20371510]

Kotzbauer PT, et al. , 2001. Lewy body pathology in Alzheimer‘s disease. J. Mol. Neurosci. 17, 225–232. [PubMed: 11816795]

Kulkarni SK, et al. , 2007. Elevated zero maze: a paradigm to evaluate antianxiety effects of drugs. Methods Find. Exp. Clin. Pharmacol 29, 343–348. [PubMed: 17805436]

Lemmens MA, et al. , 2011. Age-related changes of neuron numbers in the frontal cortex of a transgenic mouse model of Alzheimer‘s disease. Brain Struct. Funct 216, 227–237. [PubMed: 21409417]

Lesage S, et al. , 2013. G51D alpha-synuclein mutation causes a novel parkinsonianpyramidal syndrome. Ann. Neurol 73, 459–471. [PubMed: 23526723]

Lindzey G, et al. , 1961. Social dominance in inbred mouse strains. Nature 191, 474–476. [PubMed: 13762409]

Luk KC, et al. , 2012a. Pathological alpha-synuclein transmission initiates Parkinson-like neurodegeneration in nontransgenic mice. Science 338, 949–953. [PubMed: 23161999]

Luk KC, et al. , 2012b. Intracerebral inoculation of pathological alpha-synuclein initiates a rapidly progressive neurodegenerative alpha-synucleinopathy in mice. J. Exp. Med 209, 975–986. [PubMed: 22508839]

Magen I, et al. , 2012. Cognitive deficits in a mouse model of pre-manifest Parkinson‘s disease. Eur. J. Neurosci 35, 870–882. [PubMed: 22356593]

Magen I, et al. , 2015. Social cognition impairments in mice overexpressing alpha-synuclein under the Thy1 promoter, a model of pre-manifest Parkinson‘s disease. J. Park. Dis 5, 669–680.

Masuda-Suzukake M, et al. , 2013. Prion-like spreading of pathological alpha-synuclein in brain. Brain 136, 1128–1138. [PubMed: 23466394]

Masuda-Suzukake M, et al. , 2014. Pathological alpha-synuclein propagates through neural networks. Acta Neuropathol. Commun 2, 88. [PubMed: 25095794]

Mattila PM, et al. , 2000. Alpha-synuclein-immunoreactive cortical Lewy bodies are associated with cognitive impairment in Parkinson‘s disease. Acta Neuropathol. 100, 285–290. [PubMed: 10965798]

Muller J, et al. , 1997. Functional inactivation of the lateral and basal nuclei of the amygdala by muscimol infusion prevents fear conditioning to an explicit conditioned stimulus and to contextual stimuli. Behav. Neurosci 111, 683–691. [PubMed: 9267646]

Osterberg VR, et al. , 2015. Progressive aggregation of alpha-synuclein and selective degeneration of lewy inclusion-bearing neurons in a mouse model of parkinsonism. Cell Rep. 10, 1252–1260. [PubMed: 25732816]

Parkkinen L, et al. , 2005. Alpha-synuclein pathology does not predict extrapyramidal symptoms or dementia. Ann. Neurol 57, 82–91. [PubMed: 15562510]

Patterson JR, et al. , 2019. Time course and magnitude of alpha-synuclein inclusion formation and nigrostriatal degeneration in the rat model of synucleinopathy triggered by intrastriatal alpha-synuclein preformed fibrils. Neurobiol. Dis 130, 104525. [PubMed: 31276792]

Paumier KL, et al. , 2015. Intrastriatal injection of pre-formed mouse alpha-synuclein fibrils into rats triggers alpha-synuclein pathology and bilateral nigrostriatal degeneration. Neurobiol. Dis 82, 185–199. [PubMed: 26093169]

Paylor R, et al. , 1994. DBA/2 and C57BL/6 mice differ in contextual fear but not auditory fear conditioning. Behav. Neurosci 108, 810–817. [PubMed: 7986374]

Phillips RG, LeDoux JE, 1992. Differential contribution of amygdala and hippocampus to cued and contextual fear conditioning. Behav. Neurosci 106, 274–285. [PubMed: 1590953]

Polinski NK, et al. , 2018. Best practices for generating and using alpha-Synuclein pre-formed fibrils to model Parkinson‘s disease in rodents. J. Park. Dis 8, 303–322.

Polymeropoulos MH, et al. , 1997. Mutation in the alpha-synuclein gene identified in families with Parkinson‘s disease. Science 276, 2045–2047. [PubMed: 9197268]

Rey NL, et al. , 2018. Spread of aggregates after olfactory bulb injection of alpha-synuclein fibrils is associated with early neuronal loss and is reduced long term. Acta Neuropathol. 135, 65–83. [PubMed: 29209768]

Rozeske RR, et al. , 2015. Prefrontal neuronal circuits of contextual fear conditioning. Genes Brain Behav. 14, 22–36. [PubMed: 25287656]

Russell A, et al. , 2014. The impact of dementia development concurrent with Parkinson‘s disease: a new perspective. CNS Neurol. Disord. Drug Targets 13, 1160–1168. [PubMed: 25230219]

Rutherford NJ, et al. , 2016. Novel antibodies to phosphorylated alpha-synuclein serine 129 and NFL serine 473 demonstrate the close molecular homology of these epitopes. Acta Neuropathol. Commun 4, 80. [PubMed: 27503460]

Sacino AN, et al. , 2013. Induction of CNS alpha-synuclein pathology by fibrillar and non-amyloidogenic recombinant alpha-synuclein. Acta Neuropathol. Commun 1, 38. [PubMed: 24252149]

Schmitz C, 1998. Variation of fractionator estimates and its prediction. Anat. Embryol. (Berl) 198, 371–397. [PubMed: 9801058]

Schneider B, Koenigs M, 2017. Human lesion studies of ventromedial prefrontal cortex. Neuropsychologia 107, 84–93. [PubMed: 28966138]

Singleton AB, et al. , 2003. alpha-Synuclein locus triplication causes Parkinson‘s disease. Science 302, 841. [PubMed: 14593171]

Sugita S, et al. , 2002. NECABs: a family of neuronal Ca(2+)-binding proteins with an unusual domain structure and a restricted expression pattern. Neuroscience 112, 51–63. [PubMed: 12044471]

Taguchi K, et al. , 2016. Brain region-dependent differential expression of alpha-synuclein. J. Comp. Neurol 524, 1236–1258. [PubMed: 26358191]

Teffer K, Semendeferi K, 2012. Human prefrontal cortex: evolution, development, and pathology. Prog. Brain Res 195, 191–218. [PubMed: 22230628]

Trnka R, et al. , 2018. Amygdala and emotionality in Parkinson‘s disease: an integrative review of the neuropsychological evidence. Neuro Endocrinol Lett. 39, 105–110. [PubMed: 29919988]

Tucker LB, McCabe JT, 2017. Behavior of male and female C57BL/6J mice is more consistent with repeated trials in the elevated zero maze than in the elevated plus maze. Front. Behav. Neurosci 11, 13. [PubMed: 28184191]

Uchikado H, et al. , 2006. Alzheimer disease with amygdala Lewy bodies: a distinct form of alpha-synucleinopathy. J. Neuropathol. Exp. Neurol 65, 685–697. [PubMed: 16825955]

Vargas KJ, et al. , 2017. Synucleins have multiple effects on presynaptic architecture. Cell Rep. 18, 161–173. [PubMed: 28052246]

Volpicelli-Daley LA, et al. , 2011. Exogenous alpha-synuclein fibrils induce Lewy body pathology leading to synaptic dysfunction and neuron death. Neuron 72, 57–71. [PubMed: 21982369]

Volpicelli-Daley LA, et al. , 2014. Formation of alpha-synuclein Lewy neurite-like aggregates in axons impedes the transport of distinct endosomes. Mol. Biol. Cell 25, 4010–4023. [PubMed: 25298402]

Wang F, et al. , 2011. Bidirectional control of social hierarchy by synaptic efficacy in medial prefrontal cortex. Science 334, 693–697. [PubMed: 21960531]

Wang F, et al. , 2014. The mouse that roared: neural mechanisms of social hierarchy. Trends Neurosci. 37, 674–682. [PubMed: 25160682]

Wu Q, et al. , 2019. Alpha-synuclein (alphaSyn) preformed fibrils induce endogenous alphaSyn aggregation, compromise synaptic activity and enhance synapse loss in cultured excitatory hippocampal neurons. J. Neurosci 39 (26), 5080–5094. [PubMed: 31036761]

Zarranz JJ, et al. , 2004. The new mutation, E46K, of alpha-synuclein causes Parkinson and Lewy body dementia. Ann. Neurol 55, 164–173. [PubMed: 14755719]

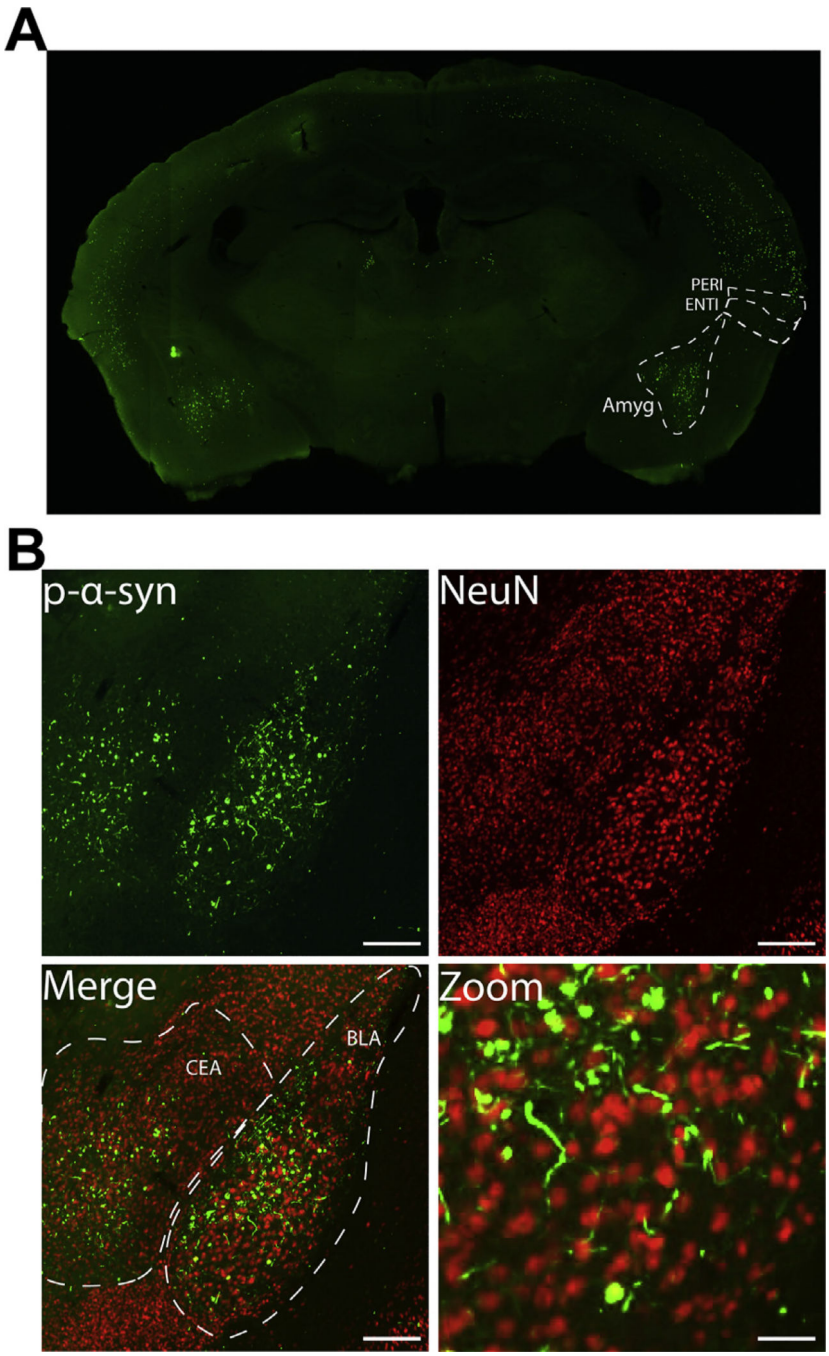

Fig. 1.

Bilateral fibril injection leads to α-synuclein inclusion formation in the basolateral and central amygdala. Mice received bilateral injections of α-syn fibrils at 3–4 months of age. A) pSer129-α-synuclein (EP1536Y) immunofluorescence from a representative coronal section showing inclusions in the basolateral and central amygdala. B) Higher magnification of immunofluorescence for pSer129-α-synuclein (green) and NeuN (red) showing inclusions in neurons in the basolateral and central nuclei of the amygdala. Scale bar = 200 μm and 50 μm (zoom). Abbreviations: Amyg = amygdala, BLA = basolateral

nucleus of the amygdala, CEA = central nucleus of the amygdala, ENTI = entorhinal cortex, PERI = perirhinal cortex. (For interpretation of the references to colour in this figure legend, the reader is referred to the web version of this article.)

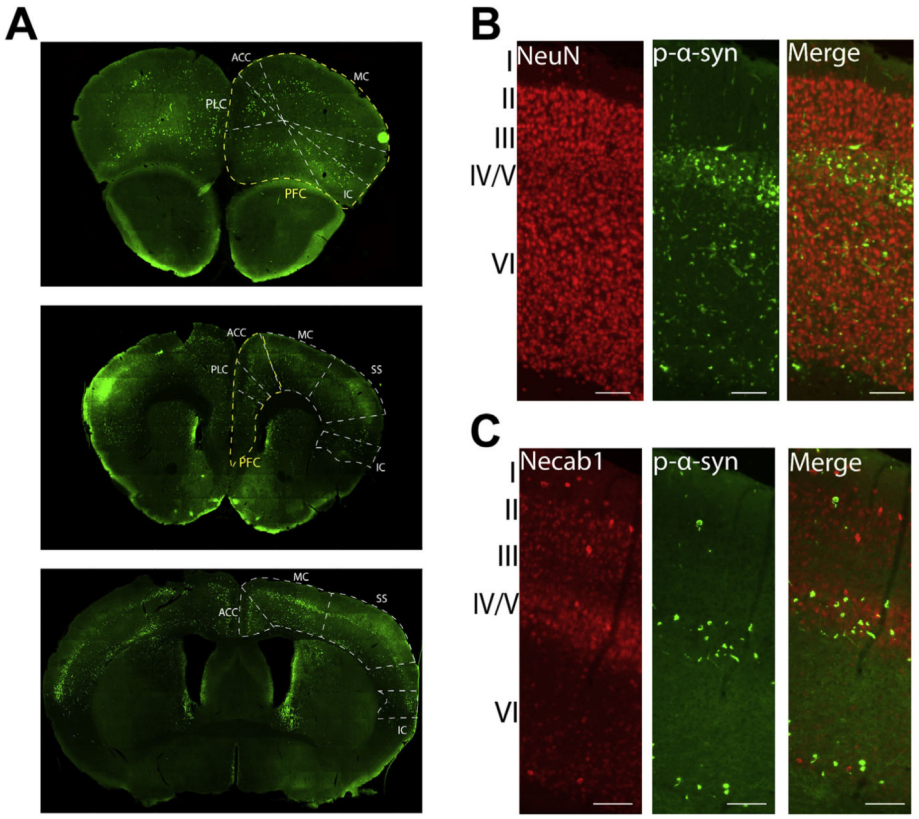

Fig. 2.

Bilateral fibril injection leads to α-synuclein inclusion formation in the cortex. Mice received bilateral injections of α-syn fibrils at 3–4 months of age. A) pSer129-α-synuclein (green; EP1536Y) shows inclusions in coronal sections of the forebrain. Yellow outlines the prefrontal cortex and white outlines other subdivisions of the cortex. B) Double-staining immunofluorescence for NeuN (red) and pSer129-α-synuclein (green; EP1536Y) shows banding pattern of inclusions in lower layers (IV/V and VI) of the motor cortex. C) Double-staining immunofluorescence for Necab1 (red) and pSer129-α-synuclein (green; 81a) shows localization of inclusions to layer IV/V. Scale bar = 100 μm. Abbreviations: ACC = anterior cingulate cortex, IC = insular cortex, MC = motor cortex, PFC = prefrontal cortex, PLC = prelimbic cortex, SS = somatosensory cortex. (For interpretation of the references to colour in this figure legend, the reader is referred to the web version of this article.)

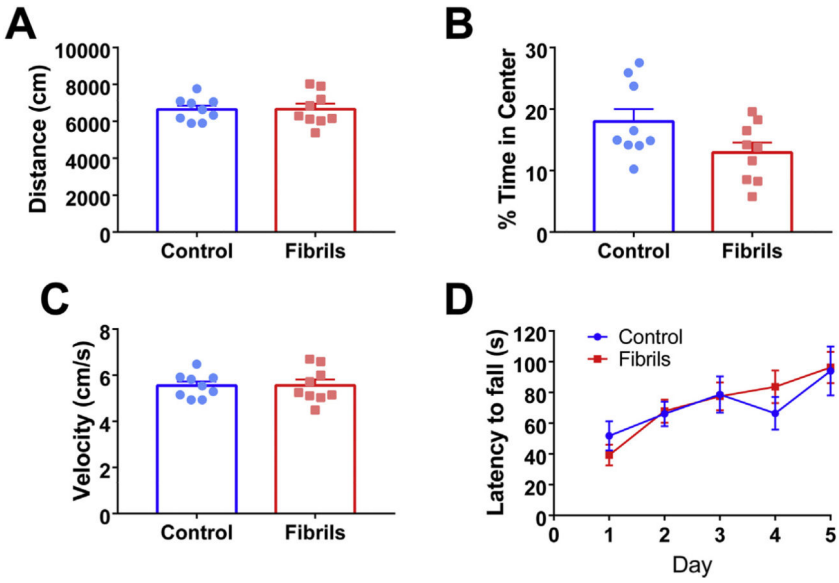

Fig. 3.

Fibril-injected mice lack overt motor deficits. Mice received bilateral injections of α-syn fibrils or PBS as a control at 3–4 months of age. Six months after injection, mice were subjected to tests of motor function. In the open field test, there were no significant differences between groups in A) distance traveled (unpaired t-test: $p = .97$, df = 16), B) percent time in center (unpaired t-test: $p = .068$, df = 16), or C) velocity (unpaired t-test: $p = .9742$, df = 16). D) Control and fibril-injected mice showed no significant difference in latency to fall on accelerating rotarod testing (repeated measures ANOVA: $p = .9044$; F(1,16) = 0.0149). Graph shows average of 3 trials per day over 5 days of testing. For all groups, N = 9.

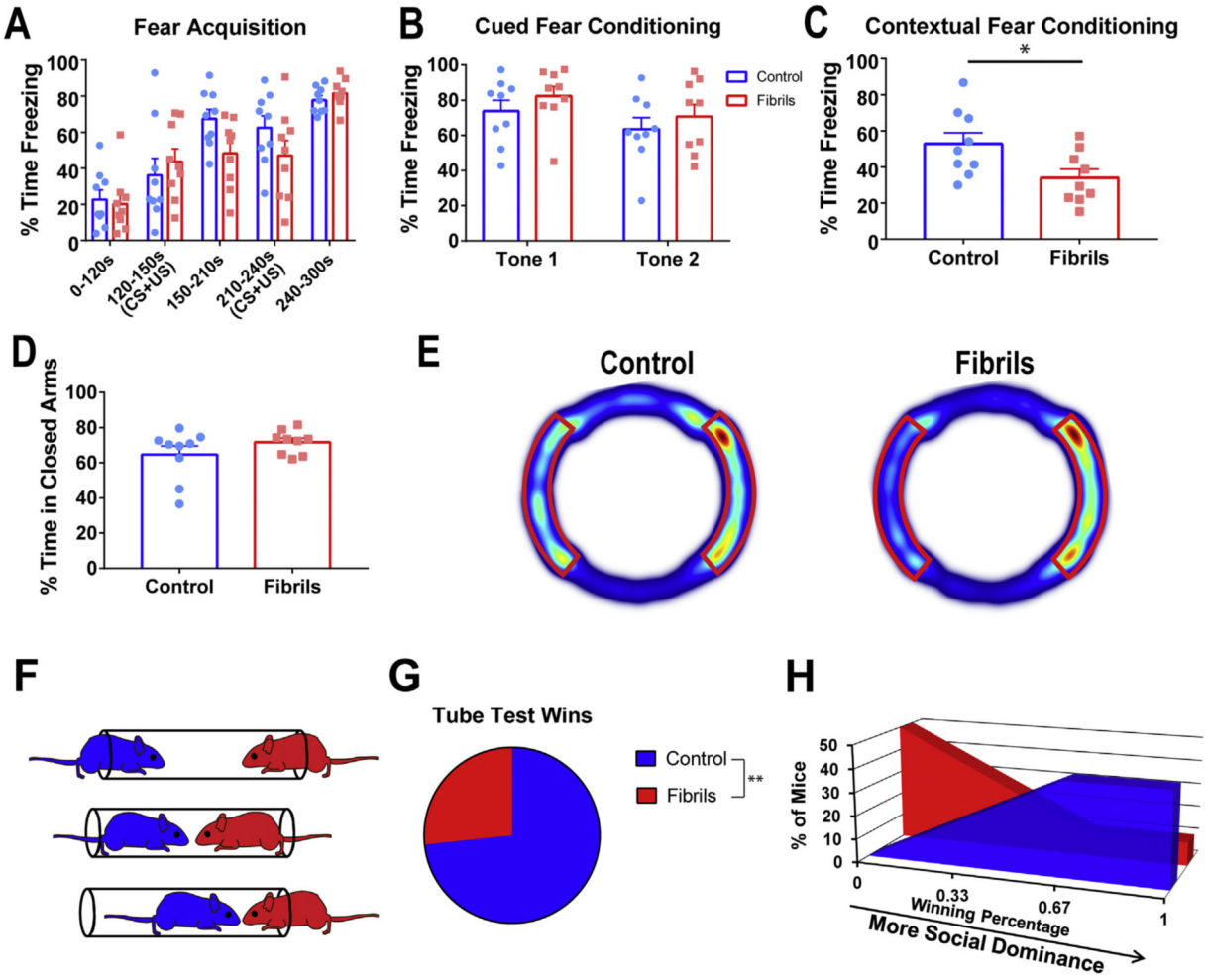

Fig. 4.

Fibril-injected mice have deficits in fear memory and social dominance. All tests were performed 6 months after control (PBS, cohort 1, A, B,C,D, E; monomer cohort 2 F,G,E) or fibril injections. A) Fibril-injected and control mice showed no difference in fear acquisition (repeated measures ANOVA: $p = .4266$, F (1,16) = 0.6656) or in B) cued fear conditioning (repeated measures ANOVA: $p = .2871$; F(1,16) = 1.213). For contextual fear conditioning, control mice froze an average of 53% and fibril-injected mice froze an average of 34% (unpaired t-test: $p = .0281$; $t = 2.414$; df = 16). D) Mice showed no significant difference in time spent in closed arms of the elevated zero maze (unpaired t-test: $p = .4117$; $t = 0.8429$; df = 16). E) Average heat maps from the elevated zero maze. Closed arms are outlined in red. F) Schematic of tube test for social dominance. Mice underwent three rounds of testing against same-sex mice from the opposite treatment group. G) Compared to control mice, fibril-injected mice exhibited a losing phenotype (binomial test: $p = .0081$) and H) the majority of fibril-injected animals won less than one round. N = 9 for all groups. *$p < .05$, **$p < .01$. (For interpretation of the references to colour in this figure legend, the reader is referred to the web version this article.)

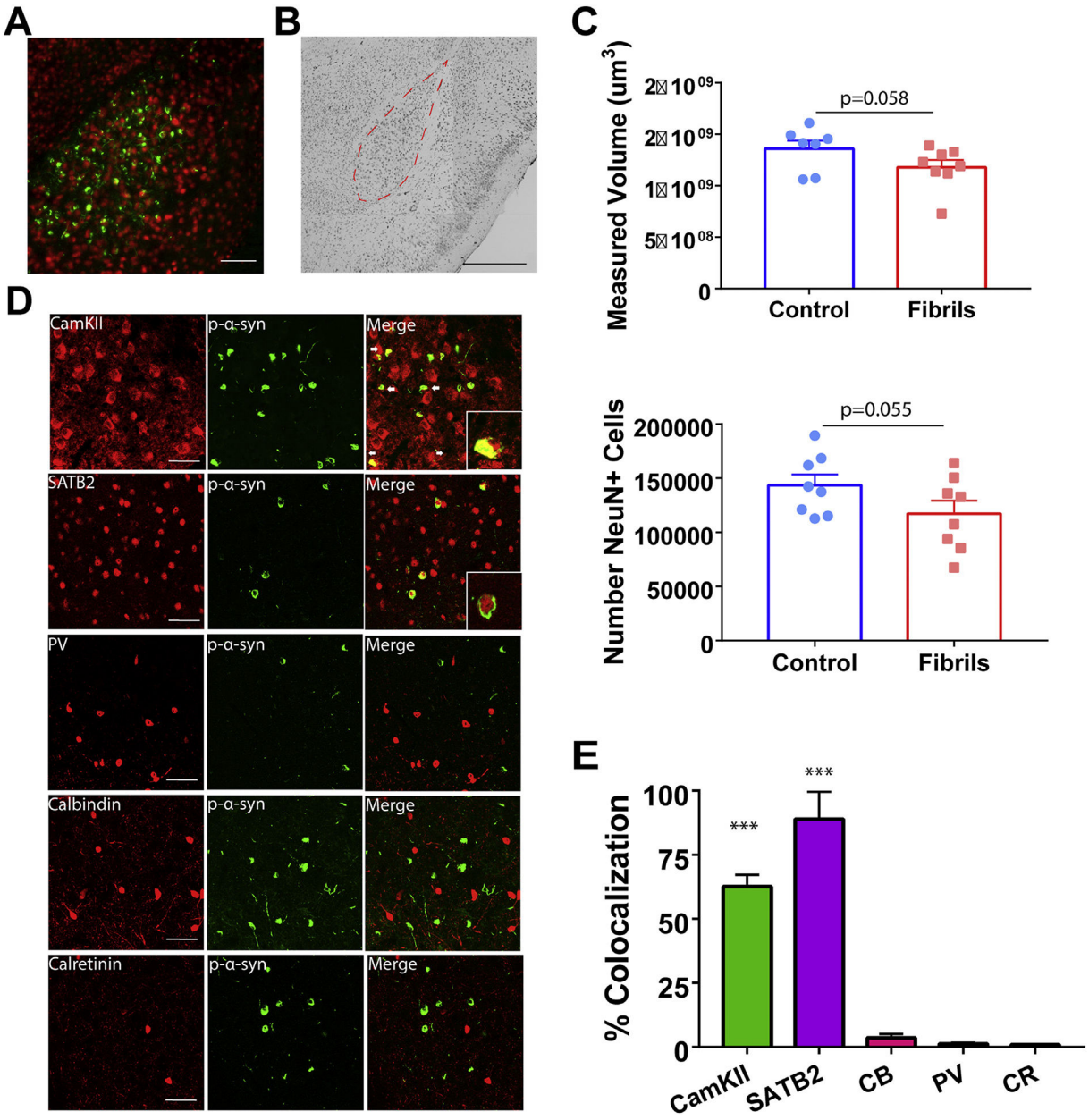

Fig. 5.

pSer129-α-Synuclein inclusions localize primarily to excitatory amygdala neurons. Mice received bilateral injections of α-syn fibrils or monomeric α-synuclein as a control. A) Immunofluorescence double-labeling for pSer129-α-synuclein (green) and NeuN (red) as a marker of neurons shows inclusions in the basolateral amygdala. B) Representative immunohistochemistry for NeuN on animals 6 months after injection with tracing for the basolateral amygdala, used for unbiased stereology. C) Unbiased stereology in the basolateral amygdala showed slight, but nonsignificant, differences in volume (N = 7–8/group; unpaired t-test: $p = .0578$; $t = 1.686$; df = 13) and neuron count (N = 7–8/group; unpaired t-test: $p = .0553$; $t = 1.703$; df = 14). D) Representative confocal images of excitatory and inhibitory markers (red) and pSer129-α-synuclein (green; EP1536Y used

for costaining with CamKII, CB, and CR; 81a used for costaining with SATB2 and PV). E) Quantification of colocalization of pSer129-α-synuclein over excitatory and inhibitory markers, normalized to pSer129-α-synuclein over NeuN (N = 3 with 3–5 images/animal; ANOVA: $p < .0001$; $F(4,40) = 62.19$. ***$p < .0001$. Scale bar = 100 μm (A), 500 μm (B), and 50 μm (D). Abbreviations: CR = calretinin, CamKII = Ca2+/calmodulin-dependent protein kinase II, CB = calbindin, PV = parvalbumin. (For interpretation of the references to colour in this figure legend legend, the reader is referred to the web version of this article.)

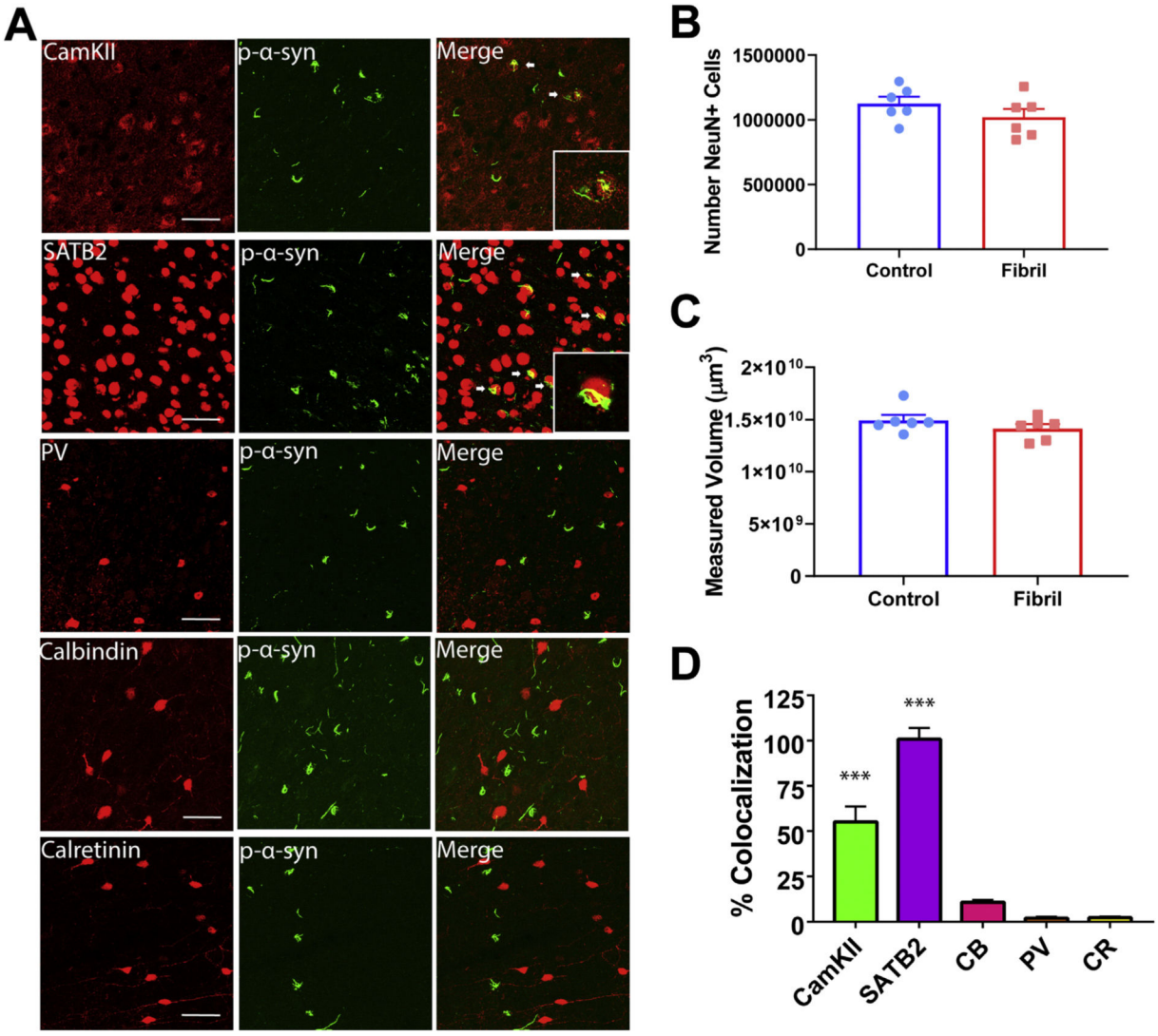

Fig. 6.

In the prefrontal cortex, p-α-synuclein inclusions localize primarily to excitatory neurons. Mice received bilateral injections of α-syn fibrils or monomeric α-synuclein as a control. A) Representative confocal images of excitatory and inhibitory markers (red) and pSer129-α-synuclein (green; EP1536Y used for costaining with CamKII, CB, and CR; 81a used for costaining with SATB2 and PV) in the prefrontal cortex. B) Unbiased volumetric estimation in the prefrontal cortex (N = 6/ group; unpaired t-test: $p = .2542$; $t = 1.210$; df = 10) C) Unbiased neuron count (N = 6/group; unpaired t-test: $p = .2338$; $t = 1.267$; df = 10). D) Quantification of colocalization of pSer129-α-synuclein over excitatory or inhibitory markers, normalized to pSer129-α-synuclein over NeuN (N = 3 with 3–5 images/mouse; ANOVA: $p < .0001$; F(4,40) = 81.54. ***$p < .0001$. Scale bar = 50 μm. Abbreviations: CR = calretinin, CamKII = Ca2+/calmodulin-dependent protein kinase II, CB = calbindin, PV = parvalbumin. (For interpretation of the references to colour in this figure legend, the reader is referred to the web version of this article.)

Table 1

Primary antibodies used for immunohistochemistry and immunofluorescence.

Primary antibody/Clone name	Catalog number	Source	Host species/Isotype/Mono or polyclonal
NeuN	MAB377	Millipore	Mouse/IgG1/Mono
pSer-129- α-syn/EP1536Y	ab168381	AbCam	Rabbit/IgG/Mono
pSer-129- α-syn/81a	825701	Biolegend	Mouse/IgG2a/Mono
Total α- and β-synuclein/EP1646Y	AB51252	AbCam	Rabbit/IgG/Mono
Necab1	PA5–54849	Invitrogen	Rabbit/IgG/Poly
CamKII	ab22609	AbCam	Mouse/IgG1/Mono
SATB2	ab92446	AbCam	Rabbit/IgG/Mono
Parvalbumin	mab1572	Millipore	Mouse/IgG1/Mono
Calbindin	C9848	Sigma-Aldrich	Mouse/IgG1/Mono
Calretinin	MAB1568	Millipore	Mouse/IgG1/Mono